Thermal stability, phase segregation, and sublimation of cesium fulleride thin films

Daniel Löffler, Patrick Weis, Sharali Malik, Artur Böttcher,*,† and Manfred M. Kappes*,‡
Institut für Physikalische Chemie, Universität Karlsruhe, Fritz-Haber-Weg 4, 76131 Karlsruhe, Germany
(Received 29 October 2007; revised manuscript received 13 February 2008; published 3 April 2008)

The topography, thermal stability, and sublimation of cesium fulleride thin films (<100 nm) prepared on highly oriented pyrolytic graphite surfaces by sequential deposition of C_{60} followed by Cs have been investigated under ultrahigh-vacuum conditions. *In situ* thermal desorption spectroscopy with mass spectrometric detection, ultraviolet photoelectron spectroscopy, and x-ray photoelectron spectroscopy, as well as *ex situ* scanning electron and scanning force microscopies, were applied. The incorporation of Cs atoms proceeds via the formation of nanoscale-sized Cs_xC_{60} grains. Weakly doped films with overall compositions of $Cs_{x<4}C_{60}$ undergo thermally induced decomposition by three-step sublimation of C_{60} and/or C_{60} containing molecular species. This is associated with three desorption peaks: α at 570 K, β at 660–720 K, and γ at 820–900 K. Peak α corresponds to C_{60} desorption from pure C_{60} regions. Sublimation peak β is associated with desorption of more strongly bound C_{60} from layers terminating Cs_xC_{60} phases ($x<4$). The ensuing saturated Cs_xC_{60} ($4 \leqslant x \leqslant 6$) phases decompose only via the sublimation of intact Cs_xC_{60} molecules. The related sublimation band γ marks the limit of the thermal stability of these phases. Its maximum shifts to higher temperature with increasing Cs doping degree x (820 K$<T<$930 K). All unsaturated Cs_xC_{60} ($x<4$) phases appear to undergo a thermally driven segregation process: $nC_{60}^{m-} \rightarrow C_{60} + mC_{60}^{n-}$ ($n<m$), resulting in the formation of Cs-free C_{60} layers terminating a saturated and conceivably homogeneous Cs_xC_{60} ($4 \leqslant x \leqslant 6$) subsurface phase.

DOI: 10.1103/PhysRevB.77.155405 PACS number(s): 78.55.Qr, 71.20.Tx, 81.05.Tp, 81.07.Bc

I. INTRODUCTION

Alkali metal fullerides have long been of interest due to their characteristic electronic properties. For example, electrical conductivity can be varied within a wide range from semiconducting up to high-temperature superconducting simply by changing the exohedral doping level.[1] The prevalent type of conductivity in different A_xC_{60} phases is governed by the relationship between electron-electron and electron-phonon interactions, which in turn depends on the stoichiometry.[2] Thermal stability and, in particular, thermally driven phase transitions are being increasingly studied in order to explain the observed temperature dependencies of several relevant physical properties (conductivity, electron susceptibility, magnetization, polymerization, etc.).

Several Cs_xC_{60} phases, notably $x=1$, 3, 4, and 6,[3] are known and their properties have been extensively studied. While having typically comparable properties to other alkali fullerides, Cs_xC_{60} phases exhibit some peculiarities due to the high Cs atom polarizability. Cs_1C_{60} appears to be stable in the cubic fcc structure at elevated temperatures (~450 K) but it spontaneously polymerizes below 350 K.[4] The high-temperature phase can be transferred into a metastable cubic symmetry by quenching it to liquid nitrogen temperature.[3] The Cs_3C_{60} phase has been found to exist in two structures, A15 and bco.[5] The Cs_4C_{60} phase exhibits *Immm* crystal symmetry at room temperature. It undergoes an orthorhombic-tetragonal transition ($Immm \rightarrow I4/mmm$) between 300 and 620 K.[6] Klupp *et al.*[7] have applied mid- and near-infrared spectroscopies to monitor thermally induced transitions in the Cs_4C_{60} phase. Molecular vibrations at 572 and 646 cm^{-1} have been found to decay within a temperature interval between 250 and 400 K, which has been interpreted in terms of an associated molecular symmetry change of the C_{60}^{-4} ions from D_{2h} into either D_{3h} or D_{5d} symmetry.[7] The saturated Cs_6C_{60} phase has been found to be stable in the bcc structure.[8]

Böttcher *et al.*[9] have addressed the role of the surface in influencing the thermal stability of Cs_xC_{60} films. Metastable deexcitation spectroscopy using He*(2^1S) atoms[10] showed pronounced changes of the valence band occurring when heating $Cs_{x<3}C_{60}$ films from 250 to 400 K. This effect was attributed to a rearrangement of Cs atoms terminating the bulk, which significantly modified the density of states at the Fermi level. It has also been suggested that Cs atoms deposited on saturated Cs_xC_{60} films of nominal composition $x=6$ form quasimetallic Cs clusters, as indicated by the unique singlet-triplet conversion behavior of the scattered He*.

Very recently, Klupp *et al.*[11] have demonstrated that a nominally homogeneous Na_2C_{60} phase actually has an inhomogeneous charge distribution on the nanoscale. These authors used infrared, ESR, NMR, and neutron scattering data to infer that the room temperature Na_2C_{60} "phase" consists of insulating C_{60} and metallic Na_3C_{60} regions of ~3–10 nm in size. Upon heating to $T>460$ K, such nanodisproportionation or segregation is thought to disappear, presumably as mediated by jump diffusion of sodium ions. Similar charge disproportionation reactions leading to segregated C_{60}^{2-} and C_{60} regions have been suggested to take place in the metastable cubic CsC_{60} phase.[12]

In spite of the immense literature on the substance class, little is known concerning the high-temperature thermal stability of alkali fullerides. In particular and to our knowledge, there is no detailed information on sublimation processes and associated vapor content. In fact, a common assumption has been that alkali fullerides decompose irreversibly and completely into poorly defined oligomeric or polymeric structures. Partly, the problem has been the lack of sufficiently sensitive methods with which to probe the gas-phase composition.

In this paper, we report on the thermal decomposition of Cs_xC_{60} thin films produced on ultrahigh-vacuum (UHV)-clean graphite surfaces—as monitored by mass spectroscopically probing the neutral species desorbed from the film surfaces. In particular, we probe sublimation spectra for various films differing by their (initial) mean Cs doping degree x. We find that Cs_xC_{60} films in the composition range studied sublime essentially completely when heated to temperatures $T \sim 930$ K. Depending on the average film composition, we observe that decomposition proceeds in up to three stages. The sublimation behavior observed in combination with ultraviolet and x-ray photoelectron spectroscopies provides evidence for thermally induced disproportionation or phase segregation reactions of the following type: $nC_{60}^{m-} \rightarrow C_{60} + mC_{60}^{n-}$ $(m > n)$, at the film surfaces.

II. EXPERIMENT

The experimental setup has been described in detail in Ref. 13. Thus, only a brief overview of the apparatus is given here. Ion beam deposition of C_{60}^+ was used to generate high purity C_{60} multilayer films on highly oriented pyrolytic graphite (HOPG) surfaces. C_{60}^+ was generated from C_{60} vapor (AlfaAesar Company, 99.5% purity) by electron-impact ionization. After off-axis extraction to remove neutrals followed by electrostatic collimation, the ion beam passed through a quadrupole mass filter set to transmit only C_{60}^+ (>99.9% mass purity). It then perpendicularly impacted on a room temperature HOPG surface (SPI Incorporation, SPI-II quality, sample size of 7×7 mm^2). The deposition of C_{60}^+ ions was carried out under fragmentation-free soft-landing conditions, as realized by applying a retarding potential to the HOPG target ($E_{kin} < 0.1$ eV/carbon atom). The deposited C_{60} load was determined by integrating the ionic current measured during deposition using a picoamperemeter (Keithley). Thick films of up to 50 MLE used in this study were generated under the following deposition conditions: surface temperature $T_{surf} = 300$ K, kinetic energy of the ions, $E_{kin} \sim 6$ eV, and ionic flux $F \sim 2 \times 10^{12}$ ion/s cm^2 (1 MLE $= 10^{14}$ cm^{-2}, corresponding to the lateral density of a hexagonally close packed C_{60} layer).

Before starting the C_{60}^+ deposition, the HOPG surface was flashed several times up to 1100 K in order to remove –OH and –C-H terminations from step edges and defect sites. During heating of the sample, the pressure did not exceed 10^{-9} mbar. The sample temperature was monitored routinely by a K-type thermocouple attached to the back side of the sample holder. Thermal desorption measurements required a more precise control of sample temperature. For this, surface temperatures were measured without mechanical contact using a radiation pyrometer (Keller, PZ20AF). The deposited C_{60} films were kept at constant temperature while being exposed to a Cs flux as emitted by a resistively heated getter source (SAES Getters SpA, Italy). The source worked at conditions which provide a constant nominal Cs flux of $\sim 10^{14}$ Cs/cm^2 s (long preheating procedure, operating current of 6 A, short source-sample distance). Typically, cesium fulleride films were prepared by Cs dosing of C_{60} layers *kept at room temperature*. For ultraviolet photoelectron spectroscopy (UPSs) spectra, we also prepared fulleride films according to the method described by Takahashi *et al.*,[14] i.e., the C_{60} films were kept at a preselected elevated temperature (up to 525 K) until completion of the doping procedure.

All operations, C_{60} film growth and Cs doping as well as the spectroscopic analyses of the samples, were conducted in UHV at a base pressure better than 5×10^{-10} mbar. Mass resolved thermal desorption spectra of neutral particles escaping from the sample were acquired using a quadrupole mass spectrometer (Extrel) equipped with an electron impact (EI) ionizer (EI energy of 70 eV). For this, a constant heating rate of 5 K/s was applied to the sample, typically over the temperature range of 300–1100 K.

The UPS spectra were taken using a hemispherical electron energy analyzer (Omicron, ESI 125) and a He I-discharge lamp ($h\nu = 21.2$ eV). The analyzer collected photoelectrons emitted into a narrow angle of $\sim 3°$ around the surface normal. All UP spectra have been taken with an electron energy resolution of 0.1 eV and a step width of 0.05 eV. The Fermi level of the HOPG substrate was used as the zero marker of the binding-energy scale. The work-function values ϕ of deposited C_{60} films have been determined by measuring the full width Δ of the UP spectra ($\phi = h\nu - \Delta$).

The concentration of Cs atoms in the Cs_xC_{60} films created was monitored by performing x-ray photoelectron spectroscopy measurements (Omicron). The photon source used was the Mg $K\alpha$ line ($h\nu = 1253.6$ eV). In the following, we denote the mean nominal value only of the doping degree by x and label the corresponding film as Cs_xC_{60}.

The topography of the Cs_xC_{60} films created was investigated *ex situ* by applying scanning electron microscopy (SEM) (LEO1530) equipped with an energy dispersive x-ray detector (EDAX Company). In several cases, HOPG surfaces resulting from desorbing the Cs_xC_{60} films by heating to 1100 K were probed by *ex situ* scanning force microscopy (AFM) (Veeco Instruments CP-II, equipped with a 5 μm scanner and using Mikromasch NSC 18 and NSC 15 cantilevers with nominal spring constants of 4.5 and 40 N/m, respectively, having an initial tip radius of 10 nm).

III. RESULTS AND DISCUSSION

A. Sublimation of cesium doped C_{60} films

1. *Distinguishable* C_{60} *local environments*

Figures 1(a) and 1(b) show typical thermal desorption measurements for cesium doped C_{60} films on HOPG. These were prepared by exposing the deposited 20 MLE C_{60} layers to $\sim 3 \times 10^{15}$ Cs atoms/cm^2 (30 s exposure to a constant flux) at room temperature. Apparently, desorption of C_{60} molecules (as monitored in the C_{60}^+ mass channel) [Fig. 1(a)] proceeds in two steps—as shown by two sublimation peaks, β and γ, centered at 700 and 850 K, respectively. This doublet suggests that film decomposition proceeds via the sequential formation of at least two different C_{60} local environments (β and γ), distinguishable by their sublimation enthalpies.

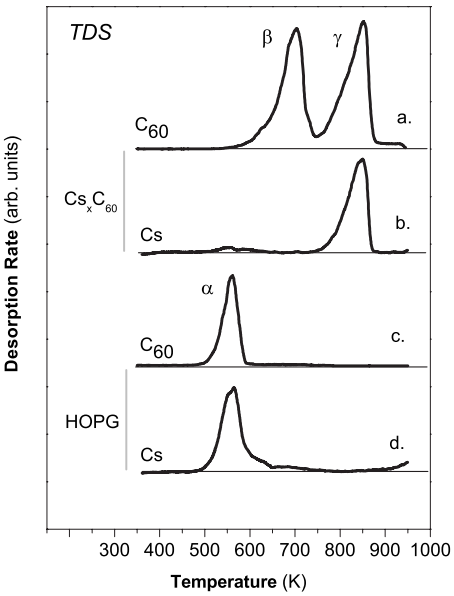

FIG. 1. Curves (a) and (b) represent mass resolved thermal desorption spectra obtained for a thick Cs_xC_{60} film, prepared by exposing a 20 MLE C_{60} deposit on HOPG to a Cs flux for 30 s; (a) C_{60}^+ (C_{60}-TD) and (b) Cs^+ (Cs-TD) mass channels: 720 and 133 amu, respectively; (c) C_{60}-TD for a pure 20 MLE thick C_{60} film deposited onto HOPG; (d) Cs TD obtained after exposing a clean HOPG surface to constant Cs flux for 5 min. All TD spectra have been taken at constant heating rate of 5 K/s.

Figure 1(b) shows a corresponding thermal desorption measurement as recorded in the Cs^+ mass channel. Only one intense peak is observed—coinciding in shape and position with peak γ, and therefore indicating that Cs^+ and C_{60}^+ signals derive from the same desorbed species. This in turn suggests that molecular Cs_yC_{60} can intactly desorb in the temperature range of 800–900 K. Note that we did not observe any ions other than Cs^+ and C_{60}^+ in the mass spectral traces. In particular, we observed no CsC_{60}^+, $Cs_2C_{60}^+$, or $Cs_3C_{60}^+$ species. Presumably, electron-impact ionization of desorbed molecular Cs_yC_{60} is associated with ionization-induced fragmentation into exclusively C_{60} and Cs cations. In the absence of a softer ionization method (e.g., photoionization), we presently cannot quantify the average Cs coverage of desorbed Cs_yC_{60}. Interestingly, density functional theory calculations on KC_{60}^+ indicate K^+ loss as the lowest energy fragmentation decay channel, whereas $K_xC_{60}^+$ ($x=2,3$) fragment via K loss. $Cs_yC_{60}^+$ is expected to behave similarly, thus rationalizing the observation of both C_{60} and Cs cations.[15]

We conclude from the thermal desorption spectroscopy (TDS) measurements that peak γ reflects sample regions having a local C_{60} environment with enough and sufficiently strongly bound Cs to allow intact Cs_yC_{60} desorption, whereas peak β reflects regions with desorbable C_{60}—which comes off the surface without simultaneous emission of $Cs^{(+)}$. For the sake of further argument, we suppose that these regions are homogeneous and therefore call them phases. It is not clear *a priori* whether phases β and γ can already coexist at room temperature or whether their formation is activated thermally. We will return to this point below.

Note that the sublimation of pure C_{60} films is already completed below 600 K,[16] as Fig. 1(c) demonstrates for a 20 MLE thick C_{60} film deposited on HOPG. Correspondingly, peak β lies *more than 100 K above* the sublimation band of pure C_{60}, which we designate as phase α in the following. Consequently, peak β cannot be assigned to pure C_{60} regions. Instead, the desorbing C_{60} species must be bound more strongly than in phase α. A first order measure of the average desorption activation energy of C_{60} from within phase β may be obtained by applying a simple Readhead analysis to the TD spectra.[17] We obtain a value of 1.9 eV for phase β, compared to 1.38 eV for pure C_{60} (band α).

On the basis of UPS and x-ray photoelectron spectroscopy (XPS) (see below), we assign phase β to C_{60} surface layers in close proximity to Cs_xC_{60} regions. In such a case, the higher binding energy relative to pure C_{60} would result from the charge-induced dipole interaction of polarizable C_{60} molecules with those Cs^+ ions terminating the Cs_xC_{60} phase. It also appears plausible that the terminating C_{60} layer might itself be partly negatively charged due to local electron transfer (see below).

2. Dependence on thin-film starting composition

We next performed a series of thermal desorption experiments using cesium doped C_{60} films fabricated by exposing multiple, equally thick (20 MLE) C_{60} layers *to different Cs doses*. Analysis of Fig. 2(a) yields that, to within experimental error, the integral C_{60}^+ intensity, and therefore the fullerene desorption yield, remains constant to within ±6%, *independent of Cs dose*. Note that AFM images of the HOPG surface, taken after performing the desorption procedure, reveal some decoration of step edges as well as on-terrace defects, both of which appear to stem from thermally induced fragmentation of the fullerene cages. Nevertheless, the near constant integral desorption yields suggest that only a small part of the film-substrate interface (much less than 1 MLE) decomposes to an irreversibly bound material upon heating.

As Fig. 2(a) shows, a very low dose of 3×10^{14} Cs/cm^2 is already sufficient to convert the single-peaked pure C_{60}-TD spectrum (peak α) into a spectrum exhibiting all three sublimation peaks, α, β, and γ. Whereas peak α rapidly decreases in intensity with progressing Cs content, peaks β and γ (first) become more intense. Band β is the most intense for the film obtained by 15 s of Cs exposure (nominal dose of 1.5×10^{15} Cs/cm^2). Beyond this Cs dose, it becomes gradually weaker—disappearing entirely in the sample prepared by 120 s exposure (nominal dose of 1.2×10^{16} Cs/cm^2). The dependence of the α, β, and γ peak intensities on Cs dose is shown in the lower panel of Fig. 2(b). The upper panel of Fig. 2(b) plots the temperatures at which peak β desorption rates are maximal (T_β). The corresponding desorption activation energies derived by applying Redhead analysis range from 1.75 to ~1.95 eV.

Figure 2(a) indicates that band γ grows stronger with increasing Cs dose until its intensity eventually saturates at exposures beyond 120 s (1.2×10^{16} Cs/cm^2). Note that, by comparison to Fig. 1(d) (TD spectrum of a pure cesium layer

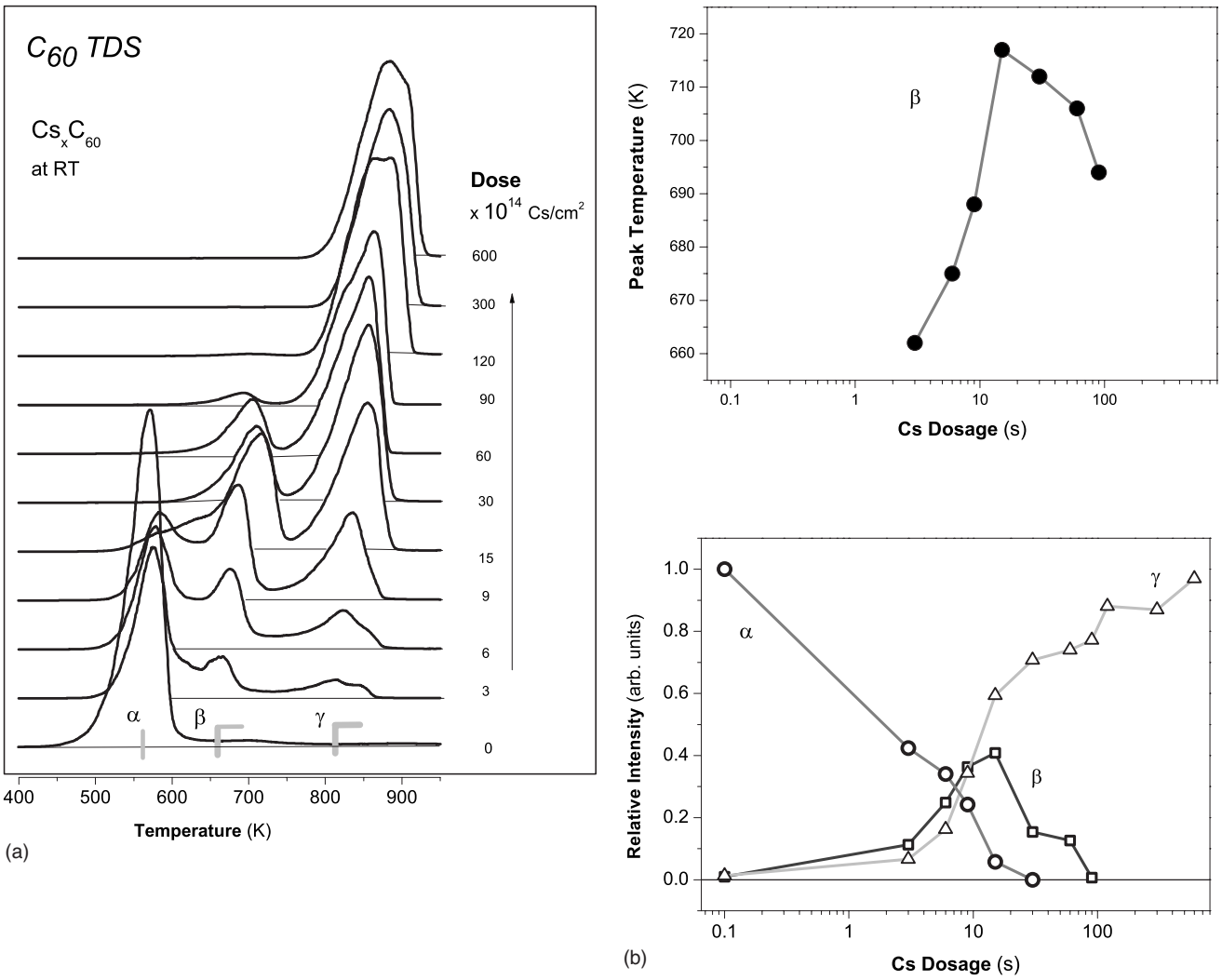

FIG. 2. (a) C_{60}-TD spectra as taken during sublimation of Cs_xC_{60} films prepared using different Cs doses. All experiments made use of the same C_{60} film thicknesses (20 MLE). Cs doping was carried out at room temperature using constant Cs flux of 10^{14} Cs/cm^2 s. (b) Evolution of the sublimation temperature of peak β upon increasing Cs exposure (upper panel). Cs dose dependence of peak β and γ intensities (lower panel).

on HOPG), Fig. 2(a) provides no indication of segregated metallic cesium islands. The fraction of incident alkali metal which sticks to the surface is apparently completely incorporated into the fullerene film or surface even for Cs exposures as high as 600 s.

A closer examination of Fig. 2(a) reveals that the sublimation band γ in fact comprises at least three distinguishable components. At low Cs doses, two components γ_1 and γ_2 centered near 820 and 850 K are present. At higher exposures (at which bands α and β are already essentially absent), a third peak γ_3 centered at 890 K dominates. On the basis of comparison to UP spectra (see below), we tentatively attribute these to distinct Cs_xC_{60} phases having $x=4$ (γ_1), 5 (γ_2), and 6 (γ_3), respectively (see below). The corresponding average desorption activation energies are 2.2, 2.3, and 2.4 eV for $x=4$, 5, and 6 phases, respectively. Note that this corresponds to an average over all subliming molecular species detected in the C_{60}^+ mass channel. Note further that whereas the Cs_4C_{60} and Cs_6C_{60} phases have been experimentally characterized well, the existence of a Cs_5C_{60} phase has only been predicted within the lattice-gas model.[18]

To summarize, at elevated temperatures, Cs doped C_{60} films (previously prepared by depositing Cs at room temperature) manifest three thermodynamically distinct C_{60} states: (α) C_{60} in pure C_{60} regions, β C_{60} cages terminating regions of Cs_xC_{60} phases ($x \leqslant 4$), and (γ) C_{60} anions as constituents of saturated Cs_xC_{60} phases ($4 \leqslant x \leqslant 6$). The TDS-based data alone do not allow distinction of whether these states are directly generated during doping or whether they are subsequently formed by heating, $\alpha \rightarrow \beta \rightarrow \gamma$. It appears plausible that the weakly doped film prepared at room temperature first consists of an ensemble of randomly distributed Cs ions embedded in the α phase. We speculate that the heating associated with a TD scan converts such a film into homogeneous phases β and γ via (presumably vertical) segregation of C_{60} molecules. Both the thermally activated diffusion of Cs and C_{60} as well as the electrostatically driven mobility of Cs^+ ions are conceivable mechanisms for supplying the necessary doping species to the unsaturated Cs_xC_{60} regions. This segregation-driven scenario is supported by the

evolution of the related C_{60}-TD peaks (α, β, and γ), as induced by increasing starting Cs content. Peak β then represents an intermediate phase, which exists only for a film with overall composition of $x \leqslant 4$. Presumably, the segregation process coincides with the appearance of the β peak, i.e., it becomes completed in a temperature region below 750 K.

Segregation into alkali-ion-rich and alkali-ion-poor regions has been theoretically predicted for a weakly doped fulleride phase, $x \leqslant 3$.[19] A lattice-gas (Ising) model incorporating a host-lattice screening mechanism in the fcc structure gives a reasonable estimation of the eutectoid temperature experimentally observed in the KC_{60} phase diagram. This model also includes interactions analogous to those postulated here for phase β, i.e., between polarizable C_{60} molecules and the nearest cations in the ionic layer terminating salt grains.

B. Electronic structure and segregation

1. Contrasting TDS and UPS measurements

UPS ($h\nu$=21.2 eV, penetration depth of ~2 MLE) is well suited for monitoring electron transfer from Cs to the lowest unoccupied molecular orbital (LUMO)-derived band of the solid C_{60} phase, as occurs in alkali fulleride formation. The formation of Cs_xC_{60} is indicated by increasing the occupation of the C_{60}-t_{1u}-derived band (fullerene LUMO band) and by gradual depletion of the C_{60} highest occupied molecular orbital (HOMO)-derived band, reflecting electron transfer and the onset of ionic interactions between $Cs^{+\delta}$ and $C_{60}^{-\delta}$.[9,20] Below, we compare UPS and TDS data in order to relate the proposed segregation process to specific electronic properties of the known Cs_xC_{60} phases potentially involved.

UP spectra recorded at room temperature for films of varying Cs content prepared by dosing Cs onto 20 MLE C_{60} layers exhibited all spectral signatures known from the literature.[9,14] Increasing Cs doping manifests itself by four main spectral modifications (not shown) relative to pristine C_{60} films: (1) weak feature located above the HOMO-derived band appears at low Cs doses, signaling gradually increasing occupation of the t_{1u}-LUMO-derived band, (2) corresponding decreased density of occupied HOMO-derived states, (3) characteristic features in the HOMO region of the C_{60} density of states (DOS) (peaks at 2.25 and 3.6 eV) showing doping dependent core-level shifts, and (4) a Cs 5p doublet (new intense peaks at ~11.9 and ~13.7 eV).

Figure 3(a) shows the corresponding evolution of the t_{1u}-LUMO-derived band—as monitored while increasing Cs content. At the lowest Cs exposures, the band profile is peaked at 0.35 eV but asymmetric, reflecting the contribution of two features, a_1 (0.35 eV) and a_2 (1 eV), respectively, which have been assigned to coexisting dimer and polymer states in the CsC_{60} phase.[21] At somewhat higher Cs doping (Cs exposures up to 9 s), the LUMO-band profile becomes more symmetric and centered at 0.55 eV (peak b). This feature has been assigned to a Cs_4C_{60} phase.[14,21] As the Cs dose is raised further, the LUMO band grows considerably in intensity and its center shifts gradually toward higher binding energy. At 600 s exposure, this shift has leveled off, leaving a band centered at 1.05 eV (peak c). The doping-induced evolution of the LUMO band shown is in perfect agreement with the data of Takahashi *et al.*[14] and De Seta *et al.*,[21] who have been able to attribute the mean doping degree x to their spectral data. Based on this assignment, peak c corresponds to a "saturated" Cs_6C_{60} phase.[14] We have also attempted to estimate the Cs concentration in this saturated phase by measuring the intensity ratio between C 1s and Cs 4d features using XPS. After including the corresponding atomic sensitivity factors, we obtained a $Cs:C_{60}$ number ratio of ~7, in good agreement with the data of De Seta *et al.*[21] Note that the doping-conditioned evolution of the LUMO band is not significantly influenced by the preparation temperature. Essentially the same LUMO-band spectra were obtained for samples prepared by 300 K as well as 450 K Cs depositions. Cs penetration into the C_{60} thin film is already very fast at room temperature—as driven by the Cs^+-$C_{60}^{-\delta}$ interaction and associated compound formation.

The lower right panel in Fig. 3(a) relates the LUMO-derived UP bands to the sublimation spectrum of a film created by 3 s Cs exposure. This can be assigned to a nominal CsC_{60} phase on the basis of its UP spectrum. However, the corresponding film exhibits all three desorption features (α, β, and γ). Desorption of C_{60} molecules (peak α) indicates that there are extended regions of solid C_{60} at (and perhaps below) the desorption onset temperature of 450 K. Peak β provides evidence for C_{60} molecules terminating Cs_xC_{60} regions at $T \leqslant 620$ K. The high-temperature γ_1 peak at 820 K has been assigned to a Cs_4C_{60} phase in the previous section. Note that the characteristic LUMO-derived UP band of Cs_4C_{60} differs clearly from that of the nascent CsC_{60} phase (b versus $a_{1,2}$). Therefore, we can infer that the original CsC_{60} phase must in fact (further) segregate or decompose into a mixture comprising the Cs_4C_{60} phase as the sample is heated.

In contrast to the weakly doped CsC_{60} phase, the upper right panel in Fig. 3(a) shows that the saturated phase (as identified by LUMO peak c and the lowest value of the work function) is characterized by only *one* very strong sublimation band, γ. There is no trace of phase β. The γ feature consists of two poorly distinguishable components located at 850 and 890 K, i.e., γ_2 and γ_3 peaks, which we have attributed to Cs_5C_{60} and Cs_6C_{60}. Thus, the Cs saturated film completely decomposes within only one broad sublimation band near 890 K, whereas the weakly doped film decomposes by emission of C_{60} molecules in three different channels, α, β, and γ. Consequently, our TDS-based identification of the relevant C_{60} states in the doped films is supported by the corresponding evolution of the LUMO-derived state with increasing doping degree.

2. Work functions and film heterogeneity

The increasing content of Cs in Cs_xC_{60} films also manifests itself by reduction in mean work function. However, as shown in the upper panel of Fig. 3(b), the corresponding secondary-electron flanks generally exhibit *two* well-defined steps, which indicate that the surfaces consist of two (or more) components, discernible by their different local work functions ($\phi_A < \phi_B$). The lower panel in Fig. 3(b) indicates that whereas ϕ_B decreases from 4.7 eV for pure C_{60} down to

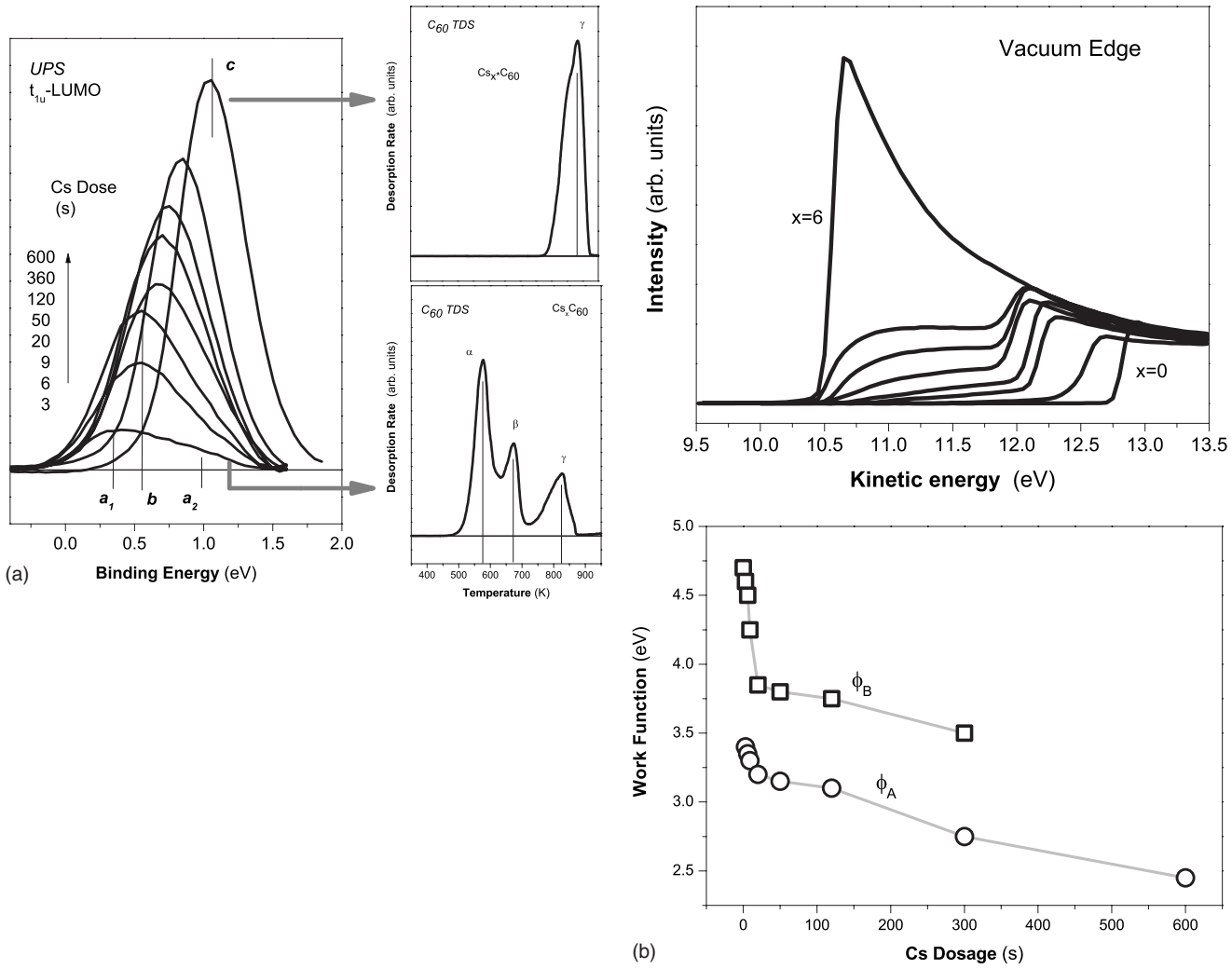

FIG. 3. (a) t_{1u}-LUMO regions of UP (21.2 eV) spectra recorded for Cs_xC_{60} films created by exposing 20 MLE C_{60} to increasing Cs doses (at room temperature). The insets at the right side show C_{60}-TD spectra taken for films corresponding to the lowest and highest Cs doses used (see arrows). (b) Secondary-electron edge (vacuum level) as monitored by UPS vs increasing Cs dose [same films as in (a)] (upper panel). The kinetic energy axis has been shifted by 8.2 eV to account for the bias intentionally applied to the sample. Note the presence of two clearly defined steps in the spectra. The lower panel shows the corresponding work functions which we assign to low-work-function $Cs_{x>4}C_{60}$ grains (ϕ_A) embedded in high-work-function $Cs_{x<4}C_{60}$ regions (ϕ_B).

3.6 eV for a near-saturated film, ϕ_A spans a range between 3.45 and 2.45 eV. Apparently, the two components remain well distinguishable over the whole doping range. Note that we can exclude the presence of metallic Cs islands on the basis of the TDS measurements as well as by comparing the ϕ_A values of the saturated film (2.45 eV) with that known for deposited Cs metal layers (2.1 eV). In future work, it would be of interest to study the size and overall distribution of granular fulleride structures by photoemission electron microscopy (PEEM).[22]

According to the Richardson–Laue–Dushman equation,[23] the intensity of the UPS photocurrent can be expressed in terms of the $h\nu-\phi$ difference, i.e., for a constant photon energy $h\nu$, a low work function results in a high emission intensity. Consequently, the stepped edge profiles shown in Fig. 3(b) (upper panel) become more intense and change their overall shape as the Cs content in the Cs_xC_{60} grains increases. However, the intensities also depend on the relative surface areas covered by the respective domains. Overall, the vacuum edge converges toward a single steep flank at high Cs coverages. This corresponds to the saturated surface of a rather homogeneous Cs_6C_{60} phase.

Therefore, in considering the global composition assignments derived from the LUMO-derived bands [Fig. 3(a)], it is important to keep in mind that the corresponding films are heterogeneous both with regard to structure and composition for overall compositions $x<6$—under our (greater than or equal to room temperature) preparation conditions.

3. Spectral modifications on temperature change

We next explored the effect of phase β decomposition and the associated C_{60} sublimation on the electronic structure of the residue. For this, fulleride films were prepared by exposing a 20 MLE thick C_{60} film to a moderate Cs dose at room temperature. This provides a film with a mean Cs content of $x<4$, a work-function value of 3.4 eV, and a LUMO-derived

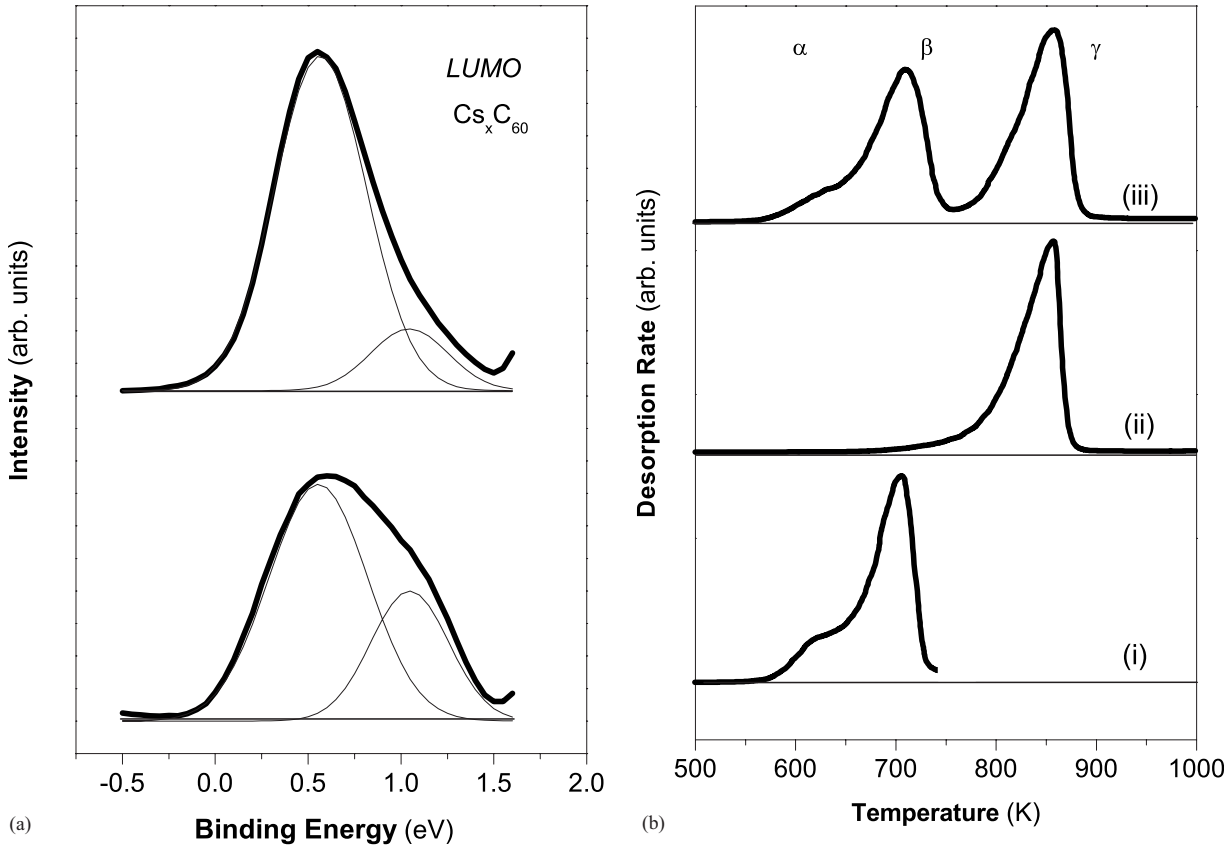

FIG. 4. (a) t_{1u}-LUMO region of the UP (21.2 eV) spectrum of a Cs_xC_{60} film of average starting composition $x<4$, taken before (lower spectrum) and after flashing the sample up to ~760 K (upper spectrum), see text for details. (b) C_{60}-TD measurements corresponding to UP spectra shown in (a): (i) $Cs_{x<4}C_{60}$ film after removal of C_{60} associated with peak β by flashing to 760 K and subsequent cooling to room temperature [cf. upper panel of (a)], (ii) C_{60} emission as observed when flashing the film (i) again but up to 1100 K, and (iii) reference behavior of a comparable $Cs_{x<4}C_{60}$ film upon heating it in one scan up to 1100 K.

UPS band comprising both a_2 and b components [Fig. 4(a)]. These electronic features are significantly changed upon heating to 750 K, which irreversibly removes the sublimable C_{60} associated with phase β. Figure 4(a) illustrates the resulting modifications of the LUMO-derived band. Whereas only traces of the a_2 peak remain, the component assigned to Cs_4C_{60}, b, clearly becomes the dominating spectral feature. We conclude that by heating the weakly doped film up to 760 K, phase segregation processes are induced, which become evident by related modifications to the electronic and thermodynamic properties. These are accompanied by the pronounced desorption of C_{60} molecules (peak β) as well as by the conversion of weakly doped $Cs_{x<4}C_{60}$ phases into the nearly saturated Cs_4C_{60} phase.

Figure 4(b) shows the corresponding C_{60}-TDS measurements: Trace (iii) reflects the overall desorption response of a film having a LUMO-derived band, as shown in Fig. 4(a), lower panel. Trace (ii) shows the TD response of an equivalently prepared film now recorded *after first removing phase* β by flashing to 750 K and then cooling to room temperature before performing the TD measurement shown. This spectrum corresponds to a sample without an a_2 peak in the LUMO band [Fig. 4(a), upper curve]. For comparison, trace (i) illustrates the C_{60} emission observed during flashing up to 750 K, as used to prepare the sample for trace (ii) measurement. A comparison of β and γ profiles in all three spectra indicates that the removal of C_{60} molecules associated with decomposition of phase β *and subsequent cooling to room temperature* does not modify the sublimation pathway of the residue. We note that essentially the same behavior is seen in TDS measurements of films having equal nominal starting compositions—independent of preparation temperature in the range of 300–525 K.

4. Renewing the β phase by further C_{60} deposition

The concept of the β phase present only at moderate overall doping degrees, $x<4$, is further supported by the following set of experiments [Fig. 5(a)]. First, a saturated film Cs_6C_{60} was prepared by Cs doping a 20 MLE thick C_{60} layer at 450 K. The corresponding TD spectrum exhibits only one strong high-temperature sublimation band, γ [lower curve in Fig. 5(a)]. An identical saturated Cs_6C_{60} film was then generated and subsequently covered by a 20 MLE thick C_{60} layer—while retaining the temperature at 450 K. The C_{60}-TD spectrum of the resulting film now exhibits two strong sublimation bands: β and γ [upper curve in Fig. 5(a)]. The absence of phase α indicates that the coating C_{60} layer has been completely converted (to primarily phase β) before reaching 450 K. We also repeated this experiment several times for less highly doped Cs_xC_{60} starting material with

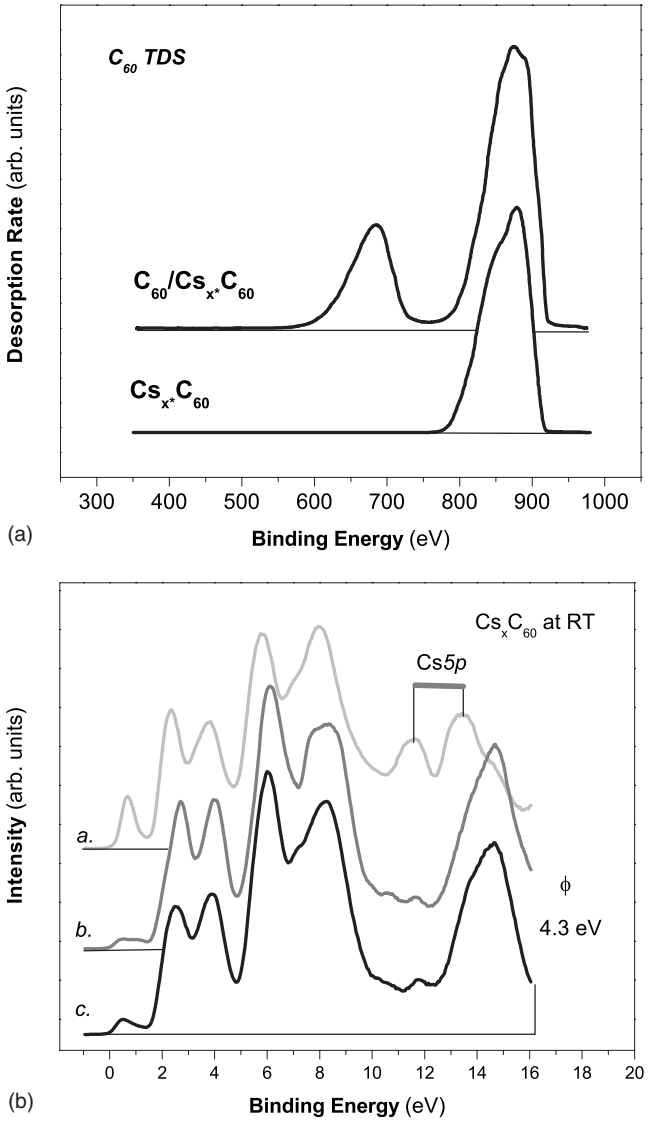

FIG. 5. (a) C_{60}-TD spectra for saturated 20 ML thick Cs_xC_{60} films of nominal starting composition $x=6$ before (lower curve) and after covering with a 20 ML thick C_{60} film at room temperature (upper curve). (b) UP spectra of a 20 MLE saturated Cs_xC_{60} film ($x=6$ nominal starting composition): (spectrum a) after preparation by room temperature Cs deposition, (spectrum b) after coverage with a nominally 50 MLE C_{60} film at room temperature, and (spectrum c) after annealing the resulting layered film at 500 K for 60 s.

analogous results: phase β appears renewable by adding C_{60} to saturated Cs_xC_{60} films. Apparently, the C_{60} layers deposited on top of Cs_6C_{60} induce considerable intermixing at the C_{60}-Cs_6C_{60} interface, leading to the creation of coexisting β and γ states. Heating results in two C_{60} sublimation peaks, β and γ.

Next, it is of interest to consider whether the conversion of on-top deposited C_{60}, as shown in Fig. 5(a), is in fact thermally activated. Figure 5(b) shows three UP spectra of a saturated Cs_6C_{60} phase (20 MLE) taken after preparing the sample (spectrum a), after covering it at room temperature with a nominally 50 ML thick C_{60} film (spectrum b), and after annealing the sandwich film at 500 K for 60 s (spectrum c). Spectrum a exhibits a fully occupied LUMO-derived band and a Cs $5p$ doublet (11.8 and 13.6 eV), which is a marker of Cs^+ ions in the outermost layer of the Cs_6C_{60} phase.[9] Spectra b and c are rather similar to each other. Compared to spectrum a, the LUMO-derived bands appear considerably weaker and broadened. However, they still exhibit significant occupation, implying that the outermost layer of both samples consists of $C_{60}^{-\delta}$ anions. In contrast to spectrum a, there are no clearly discernible Cs $5p$ features in the 11–14 eV range, indicating that Cs atoms or ions *are essentially absent* in the topmost layers. For both samples b and c, the corresponding work functions were ~4.3 eV.

5. *Topography of the* Cs_xC_{60} *surfaces*

The work-function measurements (Sec. III B 2) suggest that coexisting alkali-rich ($Cs_{x>4}C_{60}$) and alkali-poor regions ($Cs_{x<4}C_{60}$) are present on the surface of "as-prepared" alkali fulleride films (at room temperature). In order to further study this, we employed scanning-electron microscopy (SEM), to probe for the corresponding surface heterogeneity. Figure 6 in fact provides evidence for changes in surface topography upon Cs doping of a 20 MLE thick film. Note, however, that all images were taken *ex situ*, immediately after transferring the samples prepared under UHV *through air*. They are therefore subject to possible influences of oxygen or water vapor exposure. Image A shows the rather homogeneous surface of a thick C_{60} reference film. In contrast, images B and C, obtained after (increasing) Cs doping, reveal high surface heterogeneity. Image B shows the surface of a weakly doped Cs_xC_{60} film with nominal composition $x \sim 1$, corresponding to the sample represented by the right panel of Fig. 3. The whole surface is covered by ~10 nm large bright spots surrounded by halolike areas. Conceivably, the bright features reflect Cs_xC_{60} grains with higher Cs content (corresponding to lower ϕ_A in UPS-based assignment) surrounded by areas with lower Cs contents (higher ϕ_B). Image C illustrates the surface of a considerably more highly doped Cs_xC_{60} film with nominal overall composition $x<4$, i.e., a film in which two comparably intense peaks β and γ would appear in the sublimation spectra. Here, the underlying gray surface appears densely decorated by brighter granules with a rather wide size distribution ranging from 100 to 400 nm. The size of these granules scales with increasing Cs dose, conceivably reflecting segregation between a homogeneous $Cs_{x<4}C_{60}$ phase and $Cs_{x>4}C_{60}$ grains.

Note that the formation of analogous nanometer-sized islands (20–50 nm in size) has been observed by AFM upon electrochemical doping of a C_{60} films with K and Rb atoms.[24,25] This analogy suggests a common driving force for the phase segregation observed. Interestingly, recent kinetic Monte Carlo simulations evidenced a significant gap in the Madelung energy of AC_{60} and A_3C_{60} phases and consequently predicted a room temperature segregation process, which results in the coexistence of a depleted α-C_{60} phase ($x<0.1$) together with enriched A_xC_{60} grains ($x\sim3$).[24,26] These calculations also provide additional support for the ESR-based findings which indicated that the segregation process in the nominally KC_{60} phase leads to two coexisting phases: a nearly stoichiometric K_3C_{60} and a K-free C_{60}

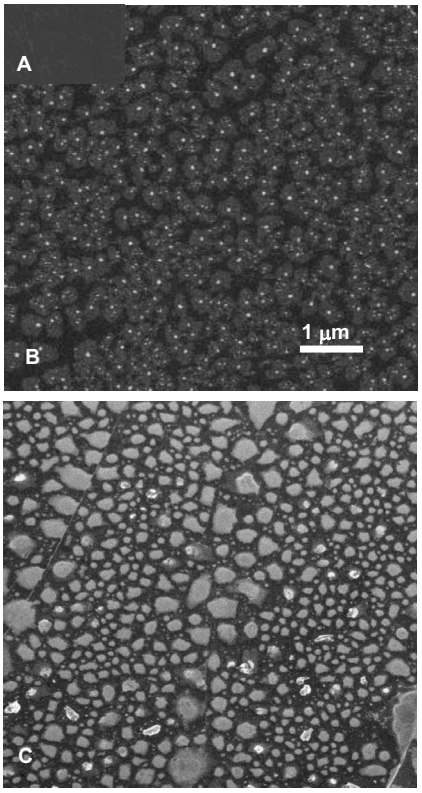

(a)

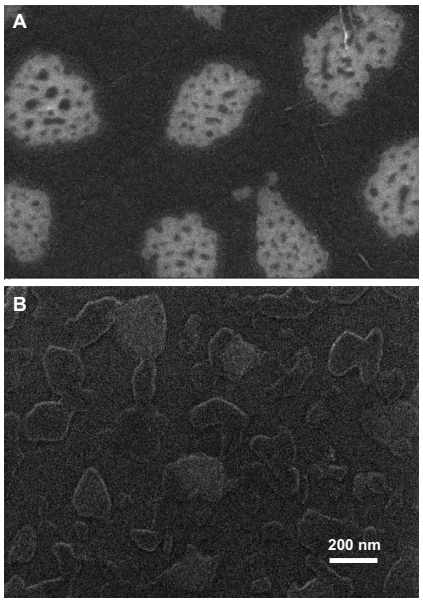

(b)

FIG. 6. (a) SEM images showing changes to the surface topography of a 20 MLE thick C_{60} film upon increasing Cs doping: (A) reference topography before Cs exposure, (B) weakly doped Cs_xC_{60} film of nominal composition $x \sim 1$, and (C) highly doped Cs_xC_{60} phase, $x < 4$. The bright areas indicate nanophase segregation and are attributed to grains of higher cesium content. (b) SEM images of a $Cs_{x<4}C_{60}$ phase taken before (image A) and after heating the sample up to 750 K (image B). This procedure removes state β and the sample appears rather homogeneous. This sample exhibits only the sublimation peak γ in the C_{60} desorption spectrum.

phase.[27] Very recently, two coexisting fulleride phases were also found in the weakly doped Na_xC_{60} films $(0 < x < 3)$.[28]

C. Nature of state β at elevated temperatures

Based on the observed granular structure of as-prepared Cs_xC_{60} films, it is tempting to attribute state β to grains of $Cs_{x<4}C_{60}$ phases, terminated by strongly polarized C_{60} molecules or even $C_{60}^{-\delta}$ anions. Due to additional interactions with Cs^+ ions incorporated in the fulleride phase, such on-top-C_{60} molecules would be more strongly bound than for a pure C_{60} phase—as is in fact observed for the β peak. However, it is not clear whether the granular structure of the $Cs_{x<4}C_{60}$ phase seen at room temperature survives when the sample is heated to the β peak sublimation temperature. In fact, the opposite behavior might be expected based on several literature reports indicating formation of homogeneous fulleride films at temperatures higher than 600 K.[27,28] In order to explore this further, we recorded SEM images of a highly doped surface before and after heating to 730 K, images A and B in Fig. 6(b), respectively. Evidently, such heating converts an initially heterogeneous surface into a more homogeneous one. Taken together with the experiments illustrated in Fig. 5, one can speculate that at elevated temperatures, the topmost layers of such films exhibit significantly different compositions than the underlying regions. Specifically, during β-C_{60} desorption, a laterally quite homogeneous fulleride film may be terminated by C_{60} molecules in neutral and/or anionic states. C_{60} emerging from the bulk and desorbing at temperatures up to 730 K would then constitute peak β. In this scenario, the steady-state lateral concentration of surface C_{60} species would reflect a delicate balance between "transport-to-surface" and desorption rates. Continued removal of β-C_{60} would lead to a gradual densification of the remaining homogeneous fulleride film while raising the mean doping degree from $Cs_{x \leqslant 4}C_{60} \rightarrow Cs_{x \geqslant 4}C_{60}$. Eventually, the saturated fulleride phase, $Cs_{x \geqslant 4}C_{60}$, would be reached, having sufficiently strongly bound C_{60} such that sublimation ceases—resuming only at considerably higher temperatures (820–930 K) via emission of intact Cs_yC_{60} molecules.

IV. SUMMARY

Thin-film cesium fullerides have been created under ultrahigh-vacuum conditions by exposing C_{60} multilayers on HOPG substrates to a moderate flux of thermal-energy Cs atoms at various surface temperatures ranging from 300 to 450 K. *In situ* UPS, XPS, and TDS, as well as *ex situ* SEM, measurements suggest that such Cs doping at room temperature generates layers which are inhomogeneous on the micro- to the nanoscale. These comprise cesium fulleride (Cs_xC_{60}) grains of various compositions interspersed with pure C_{60} regions.

Thermal decomposition of weakly Cs doped films (of average starting composition of CsC_{60}) is accompanied by desorption of C_{60} cages and ionically bound Cs_yC_{60} clusters. Depending on the starting composition, desorption occurs within three separate temperature intervals, as determined by

mass resolved TDS measurements: (α) a C_{60} emission peak at 570 K originates from unperturbed (i.e., pure) C_{60} island regions, (β) emission of C_{60} in the temperature range of 660–720 K is attributed to desorption of more strongly bound C_{60} terminating the perimeter or surface of a Cs_xC_{60} phase (with $x<4$), and (γ) emission in the range of 820–930 K is associated with the desorption of Cs_yC_{60}, originating from the decomposition of highly doped or saturated Cs_xC_{60} regions (with $x=4-6$). Desorbing Cs_yC_{60} species fragment completely upon electron-impact ionization which precluded the determination of average Cs coverage (y).

Moderately doped fulleride films of overall starting composition $x<4$ decompose via β and γ emissions without α emission. Saturated Cs_xC_{60} films with averages $x=4$, 5, and 6 decompose solely via γ emission. For all Cs_xC_{60} films, independent of the mean doping degree, the last stage of decomposition is associated with the desorption of molecular Cs_yC_{60} species. This is complete by 930 K (leaving an essentially bare HOPG).

Thus, our sublimation experiments suggest that the C_{60} cages within the Cs fulleride films prepared in this study can have three very different kinds of molecular environments: (1) molecular solids comprising neutral C_{60} surrounded by other C_{60} cages, which interact with each other via weak van der Waals forces, (2) C_{60} which is strongly polarized and/or partially charged ($C_{60}^{-\delta}$ where $\delta<1$) as a result of interaction with the surface of a rather homogenized Cs_xC_{60} phase, and (3) C_{60}^{-x} ions surrounded by x Cs^+ ions.

The sublimation channel β, which is at its most intense for moderately doped films having starting compositions of $x=1-3$, is an indicator of phase segregation processes of the following type: $nC_{60}^{m-} \rightarrow C_{60}+mC_{60}^{n-}$, with $n>m$), as occurring spontaneously during doping of the film at room temperature. As indicated by UPS vacuum level measurements and inferred from *ex situ* SEM, the applied heating procedure is associated with some further segregation-induced mass transport and local composition changes. Such processes could not be directly followed with the methods applied here. PEEM could be usefully applied to this in the future. Certainly, the β peak, in combination with our UPS measurements, implies that the conversion Cs_xC_{60} ($x<4$) $\rightarrow C_{60}+Cs_xC_{60}$ ($x \geqslant 4$) is complete by $T=730$ K.

The observed redistribution of cesium ions is a consequence of the associated thermodynamics (and mass transport kinetics). Apart from the relative stabilities of the fulleride phases involved, there are additional electrostatic contributions to the overall energetics. This is illustrated by Fig. 5(b), which shows that at least to within the penetration depth of UPS [~1–2 ML (monolayer)], the surface of a 50 ML C_{60} layer deposited on top of a saturated fulleride phase does not contain any measurable cesium—both before and after thermal annealing. However, the corresponding UP spectra show the presence of surface $C_{60}^{-\delta}$. Consequently, spontaneous electron transfer occurs at the interface between low-work-function subsurface Cs_xC_{60} layers and high electron affinity outermost C_{60}. This may lead to a local contact potential. It seems likely that such fields also influence the transport of Cs^+. In future work, it will be of interest to probe the resulting dynamic processes more directly.

ACKNOWLEDGMENTS

This work was supported by the Deutsche Forschungsgemeinschaft (DFG) as administered by the Karlsruhe Cluster of Excellence on Functional Nanostructures (CFN). We thank N. Stürzl for help with AFM measurements of HOPG surfaces after fulleride desorption.

*Corresponding authors.
†artur.boettcher.chemie.uni-karlsruhe.de
‡manfred.kappes.chemie.uni-karlsruhe.de

[1] A. F. Hebard, M. J. Rosseinsky, R. C. Haddon, D. W. Murphy, S. H. Glarum, T. T. M. Palstra, A. P. Ramirez, and A. R. Kortan, Nature (London) **350**, 600 (1991).
[2] K. Tanigaki, I. Hirosawa, T. W. Ebbesen, J. Mizuki, Y. Shimakawa, Y. Kubo, J. S. Tsai, and S. Kuroshima, Nature (London) **356**, 419 (1992); M. J. Rosseinsky, D. W. Murphy, R. M. Fleming, R. Tycko, A. P. Ramirez, T. Siegrist, G. Dabbagh, and S. E. Barrett, *ibid.* **356**, 416 (1992).
[3] V. Brouet, H. Alloul, and L. Forró, Phys. Rev. B **66**, 155123 (2002).
[4] O. Chauvet, G. Oszlànyi, L. Forró, P. W. Stephens, M. Tegze, G. Faigel, and A. Jànossy, Phys. Rev. Lett. **72**, 2721 (1994).
[5] S. Saito, K. Unemoto, S. G. Louie, and M. L. Cohen, Solid State Commun. **130**, 335 (2004).
[6] P. Dahlke, P. F. Henry, and M. J. Rosseinsky, J. Mater. Chem. **8**, 1571 (1998).
[7] G. Klupp, K. Kamarás, N. M. Nemes, C. M. Brown, and J. Leão, Phys. Rev. B **73**, 085415 (2006).
[8] O. Zhou, J. E. Fisher, N. Coustel, S. Kycia, Q. Zhu, A. R. McGhie, W. J. Romanow, J. P. McCauley, Jr., A. B. Smith III, and D. E. Cox, Nature (London) **351**, 462 (1991).
[9] A. Böttcher, S. Fichtner-Endruschat, and H. Niehus, Surf. Sci. **376**, 151 (1997).
[10] A. Böttcher, A. Morgante, R. Grobecker, T. Greber, and G. Ertl, Phys. Rev. B **49**, 10607 (1994).
[11] G. Klupp, P. Matus, D. Quintavalle, L. F. Kiss, É. Kováts, N. M. Nemes, K. Kamarás, S. Pekker, and A. Jánossy, Phys. Rev. B **74**, 195402 (2006).
[12] V. Brouet, H. Alloul, F. Quere, G. Baumgartner, and L. Forró, Phys. Rev. Lett. **82**, 2131 (1999).
[13] A. Böttcher, P. Weis, A. Bihlmeier, and M. M. Kappes, Phys. Chem. Chem. Phys. **6**, 5213 (2004).
[14] T. Takahashi, T. Morimoto, and T. Yokoya, Physica C **232**, 227 (1994).
[15] P. Weis, R. D. Beck, G. Bräuchle, and M. M. Kappes, J. Chem. Phys. **100**, 5684 (1994).
[16] H. Ulbricht, G. Moos, and T. Hertel, Phys. Rev. Lett. **90**, 095501 (2003).
[17] P. H. Redhead, Vacuum **12**, 203 (1962).
[18] G. Szabó and L. Udvardi, J. Phys.: Condens. Matter **10**, 4211 (1998).

[19] L. Udvardi and G. Szabó, J. Phys.: Condens. Matter **8**, 10959 (1996).
[20] P. J. Benning, F. Stepniak, and J. H. Weaver, Phys. Rev. B **48**, 9086 (1993).
[21] M. De Seta, L. Petaccia, and F. Evangelisti, J. Phys.: Condens. Matter **8**, 7221 (1996).
[22] W. Engel, M. E. Kordesh, H. H. Rotermund, S. Kubala, and A. von Oertzen, Ultramicroscopy **36**, 148 (1999).
[23] L. L. Jensen, D. W. Feldman, N. A. Moody, and P. G. O'Shea, J. Appl. Phys. **99**, 124905 (2006).
[24] A. Touzik, H. Hermann, and K. Wetzig, J. Chem. Phys. **120**, 7131 (2004).
[25] P. Janda, T. Krieg, and L. Dunsch, Adv. Mater. (Weinheim, Ger.) **10**, 1434 (1998).
[26] A. Touzik, H. Hermann, and K. Wetzig, Phys. Rev. B **66**, 075403 (2002).
[27] G. Faigel, G. Bortel, M. Tegze, L. Granasy, S. Pekker, G. Oszlanyi, O. Chauvet, G. Baumgartner, L. Forro, P. W. Stephens, G. Mihaly, and A. Janossy, Phys. Rev. B **52**, 3199 (1995).
[28] J. Schiessling, I. Marenne, L. Kjeldgaard, and P. Rudolf, Surf. Sci. **601**, 3933 (2007).